


RESEARCH

Open Access



# Optimizing a CRISPR-Cpf1-based genome engineering system for *Corynebacterium glutamicum*

Jiao Zhang<sup>1</sup>, Fayu Yang<sup>1</sup>, Yunpeng Yang<sup>1,2</sup>, Yu Jiang<sup>3</sup> and Yi-Xin Huo<sup>1,2\*</sup> 

## Abstract

**Background:** *Corynebacterium glutamicum* is an important industrial strain for the production of a diverse range of chemicals. Cpf1 nucleases are highly specific and programmable, with efficiencies comparable to those of Cas9. Although the *Francisella novicida* (Fn) CRISPR-Cpf1 system has been adapted for genome editing in *C. glutamicum*, the editing efficiency is currently less than 15%, due to false positives caused by the poor targeting efficiency of the crRNA.

**Results:** To address this limitation, a screening strategy was developed in this study to systematically evaluate crRNA targeting efficiency in *C. glutamicum*. We quantitatively examined various parameters of the *C. glutamicum* CRISPR-Cpf1 system, including the protospacer adjacent motif (PAM) sequence, the length of the spacer sequence, and the type of repair template. We found that the most efficient *C. glutamicum* crRNA contained a 5'-NYTV-3' PAM and a 21 bp spacer sequence. Moreover, we observed that linear DNA could be used to repair double strand breaks.

**Conclusions:** Here, we identified optimized PAM-related parameters for the CRISPR-Cpf1 system in *C. glutamicum*. Our study sheds light on the function of the FnCpf1 endonuclease and Cpf1-based genome editing. This optimized system, with higher editing efficiency, could be used to increase the production of bulk chemicals, such as isobutyrate, in *C. glutamicum*.

**Keywords:** *Corynebacterium glutamicum*, CRISPR-Cpf1, PAM, crRNA, Linear template, Isobutyrate

## Background

*Corynebacterium glutamicum* is a facultatively anaerobic Gram-positive asporogenic bacterium with short rod-like cells that is widely distributed in soil. Generally recognized as safe, *C. glutamicum* is non-pathogenic and does not produce endotoxins [1, 2]. It has been used in fermentation for over 50 years. Under anaerobic conditions, *C. glutamicum* can efficiently convert glucose to various amino acids [3, 4], organic acids [5], higher alcohols [6], and polymers [7]. Traditional genetic engineering strategies in *C. glutamicum* rely on a *SacB*-based suicide vector [8]. This process is time-consuming and inefficient,

with a false-positive rate of 20–40% [8–11]. CRISPR-Cpf1 has attracted much attention in the field of genome editing because it is easy to manipulate and has a low off-target rate. However, gene deletion or insertion in *C. glutamicum* using CRISPR-Cpf1 reaches editing efficiencies of only 5–15% [12]. Hence, it is of great importance to improve the editing efficiency of CRISPR-Cpf1 in *C. glutamicum*.

Double-strand breaks (DSBs) introduced by the CRISPR-Cpf1 system are lethal to most bacteria, including *C. glutamicum* [13], which lacks a non-homologous end joining mechanism. Therefore, DSBs serve as a selection pressure to enrich mutations repaired using the artificial donor DNA templates in this organism [14–18]. Since CRISPR-Cpf1-induced DSBs are lethal in *C. glutamicum*, the targeting efficiencies of crRNA are reflected by survival rates. crRNAs with low targeting efficiencies

\*Correspondence: huoyixin@bit.edu.cn

<sup>1</sup> Key Laboratory of Molecular Medicine and Biotherapy, School of Life Sciences, Beijing Institute of Technology, No. 5 South Zhongguancun Street, Beijing 100081, China

Full list of author information is available at the end of the article



cause a high rate of false positives during genome editing, which result in the survival of many wild-type cells within the population [17, 19–21].

FnCpf1 requires a single crRNA and a thymine-rich PAM. crRNA contains a 19 bp direct repeat sequence and a 23–25 bp spacer sequence [22–25]. PAM is a 2–6 bp protospacer-adjacent DNA sequence (Fig. 1a), which is recognized by Cpf1 and plays an important role in both Cpf1 binding and cleavage [26]. In the presence of a PAM, the Cpf1-crRNA complex can bind the target DNA and induce DSBs. The cleavage site of Cpf1 is affected by the length of the spacer sequence. When the spacer length is greater than or equal to 20 bp, Cpf1 tends to cut the 18th nucleotide of the non-complementary strand and the 23rd nucleotide of the target DNA complementary strand. When the spacer length is less than 20 bp [27], Cpf1 tends to cut the 14th nucleotide of the non-complementary strand. The cohesive end introduced by Cpf1 facilitates homologous recombination (HR) [28]. Taken together, the PAM and the length of the spacer sequence are key determinants of the efficiency of Cpf1-dependent genome editing.

Editing efficiency is also influenced by the type of repair template. In *C. glutamicum*, the plasmid-borne dsDNA template can be utilized to repair the DSBs via HR [29]. Although linear DNA templates could be used to repair DSBs in the genomes of *C. elegans* [30], mouse, and human cells [31] with high efficiency, the repair of DSBs in *C. glutamicum* via linear DNA has, to the best of our knowledge, not been reported.

Here, we describe a CRISPR-Cpf1 based method for iterative genome editing and metabolic engineering of *C. glutamicum*. We established a lethal reporter system to verify the targeting efficiency of the crRNA and constructed a series of crRNA plasmids to characterize their cleavage activities in *C. glutamicum*. We optimized this system with respect to PAM sequence, the length of the spacer sequence, and the type of repair templates. Finally, the central metabolic pathways of *C. glutamicum* were modified by our genome editing method to improve isobutyrate production. The findings of this study will facilitate engineering of metabolic networks for the synthesis of value-added products using *C. glutamicum*.

## Results

### Establishing a CRISPR-Cpf1-mediated genome editing system in *C. glutamicum*

Our CRISPR-Cpf1 system contained three elements: a constitutive Cpf1 expression cassette, a crRNA expression cassette and a donor DNA template for repairing the DSBs introduced by the Cpf1-crRNA complex (Fig. 1a). As shown in Fig. 1b, each cycle of editing started with the transformation plasmid, pYJ1\_S\_Δgene, expressing

crRNA or the plasmid, pYJ1\_SH\_Δgene, expressing the crRNA and donor DNA template in competent *C. glutamicum* cells. Unless repaired by HR in the presence of donor DNA templates, cells that took up a plasmid with functional crRNA were killed by Cpf1-mediated digestion. Eight colonies from a culture plate were picked and incubated in BHIS culture medium overnight and their genomic DNA was extracted individually. Gene knockout was verified by PCR, using primers that bind upstream of the 5' homologous arm and downstream of the 3' homologous arm. Mutants with the designed gene knockout were incubated at 37 °C in BHIS medium without antibiotics for plasmid curing and were then streaked on plates without antibiotics and grown at 30 °C (Fig. 1b). After confirming the loss of the plasmid, colonies were picked to prepare electrocompetent cells for the next round of editing.

To investigate the editing efficiencies of our system for gene deletion in *C. glutamicum*, the *upp* gene was chosen as the target gene, since its deletion leads to a 5-fluorouracil (5-FU)-resistant phenotype, which is convenient for screening [10]. We designed a crRNA targeting the *upp* gene and generated the plasmid, pYJ1\_S\_Δ*upp*. The repair template was inserted into pYJ1\_S\_Δ*upp* to create pYJ1\_SH\_Δ*upp*. After engineering and plating, all 5-FU-resistant colonies on the plate were assumed to be *upp* knockouts. Eight colonies were confirmed to have the *upp* gene deleted by both PCR screening and sequencing, as shown in Fig. 1c, d. The efficiency of *upp* deletion was 100%. To further evaluate the efficiency of the system, we constructed pYJ1\_SH\_Δ*crtYe/f* to delete the *crtYe/f* gene, since its deletion leads to a color change from yellow to red [32–34]. When the pYJ1\_SH\_Δ*crtYe/f* plasmid was introduced into competent *C. glutamicum* cells, approximately 17% of single colonies were correctly edited, according to their color.

### Generation of a lethal reporter system and optimization of PAM sequence for the Cpf1-mediated genome editing system

Two genes (*upp* and *crtYe/f*) were selected to verify the optimal PAM sequence of CRISPR-Cpf1, using a lethal reporter system. We systematically profiled the targeting efficiencies of crRNAs by co-expressing crRNA with Cpf1. Different crRNAs were inserted into the pYJ1 plasmid to construct a series of pYJ1\_S\_Δ*upp* or pYJ1\_S\_Δ*crtYe/f* plasmids, which targeted different PAM sequences. The plasmid, pYJ1, without crRNA insertion, was used as the control. After transformation, the survival rate of cells in the presence of a specific crRNA was calculated using the formula shown in the “Methods” section (Fig. 2a). The efficiency of crRNA targeting of

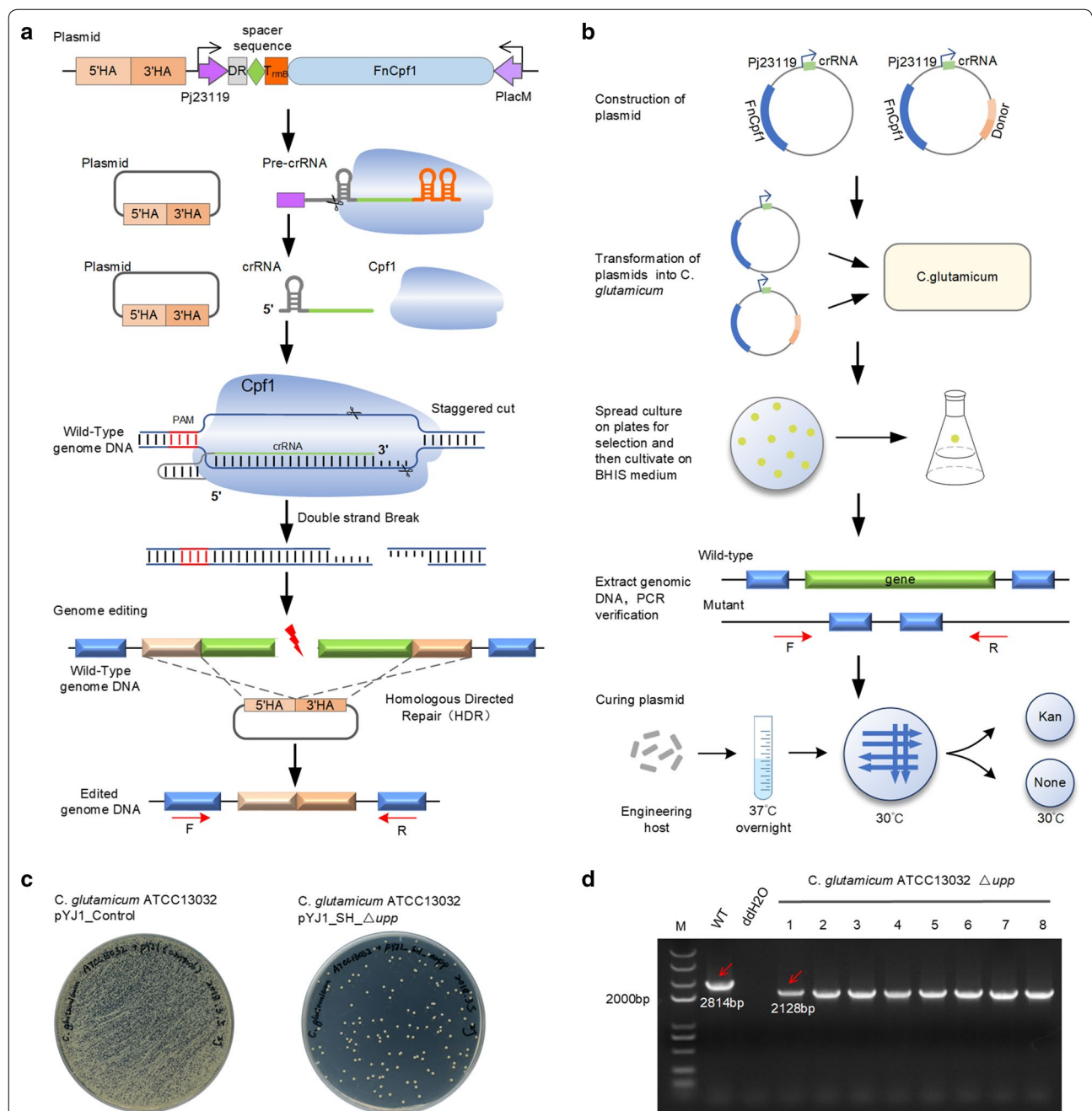
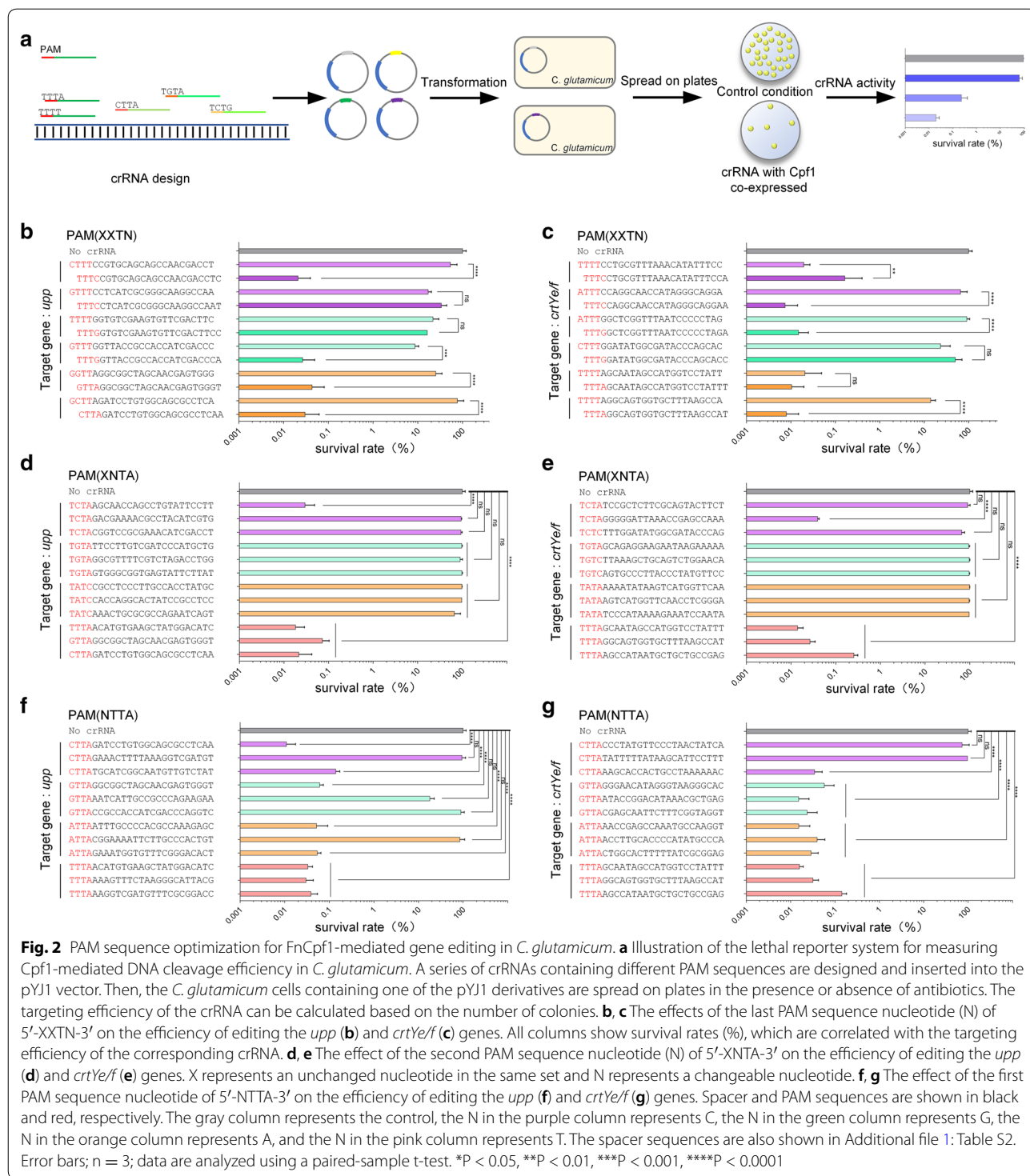


**Fig. 1** Schematic overview of the CRISPR–Cpf1-based system for iterative genome editing in *C. glutamicum*. **a** Schematic representation of genome editing using an all-in-one plasmid. The pre-crRNA is processed by Cpf1 into a mature crRNA, which then recognizes the target sequence and PAM sequence. The Cpf1–crRNA complex binds to the target site and induces a staggered cut to generate a double-strand break (DSB). The plasmid-borne template repairs the DSB through homologous recombination. The successfully edited colonies can be verified by PCR using the F/R primers located outside of the homologous arms. **b** A schematic representation of the procedure for CRISPR–Cpf1-assisted genome editing in *C. glutamicum*. A plasmid containing Cpf1, crRNA, and the repair template and another plasmid containing Cpf1 and crRNA are constructed. The two plasmids are then transformed into competent *C. glutamicum* cells and the cultures are spread on BHIS plates containing kanamycin. The single colonies are cultivated in complete medium to extract genomic DNA for PCR and DNA sequencing. The plasmid can be cured by overnight incubation in kanamycin-free medium at 37 °C and the correctly edited strain is then obtained by verifying antibiotic sensitivity. If necessary, the obtained strain can be used for the next round of editing. **c** The control (left) and edited (right) strain on the plates. The left plate is without 5-fluorouracil (5-FU) and the right plate is supplemented with 100 μM 5-FU. Under normal circumstances, the colonies on the right plate will all be positive. **d** PCR validation of *upp* gene deletion. The primers, F17/R17, used for verification, are located outside of the homologous arms. The amplified fragments are 2814 bp (wild-type) and 2128 bp (edited strain)



various PAM sequences was verified by the lethality rate of Cpf1-mediated gene editing.

The middle T is essential in the 5'-TTN-3' PAM recognized by Cpf1 [25], and crRNAs with the PAM sequence, 5'-TTT-3', have low activity in eukaryotes [35]. In order

to investigate the influence of the final "T" in the PAM on the efficiency of CRISPR-Cpf1 in prokaryotes, we targeted chromosomal *upp* or *crtYef/f*. For each gene, six sets of crRNAs were designed to contain the four-nucleotide PAM sequence, 5'-XXTN-3', where X represents



an unchanged nucleotide in a given set and N represents any nucleotide. Each crRNA set contained two crRNAs, most of which were unchanged at the first three nucleotides and differed at the fourth nucleotide in the PAM sequence. In the first and second sets, the fourth nucleotides were T and C, respectively. In the third and fourth sets, the fourth nucleotides were T and G, respectively. In the fifth and sixth sets, the fourth nucleotides were T and A, respectively. Among the spacer sequences of the two crRNAs within each crRNA set, only one nucleotide was different. crRNA spacer sequences are shown in Fig. 2b. All 12 crRNAs targeting *upp* and all 12 crRNAs targeting *crtYef* were tested in the first round of experiments.

When the last nucleotide of the PAM sequence was T, the survival rates of cells with crRNAs targeting *upp* were  $53.49 \pm 17.65\%$ ,  $17.03 \pm 2.50\%$ ,  $21.86 \pm 6.23\%$ ,  $8.64 \pm 1.48\%$ ,  $25.18 \pm 7.74\%$ , and  $76.69 \pm 23.95\%$ . When the last nucleotide of the PAM sequence was C, G, or A, the survival rates of cells with crRNAs targeting *upp* were  $0.021 \pm 0.015\%$ ,  $33.53 \pm 8.67\%$ ,  $16.27 \pm 1.58\%$ ,  $0.02 \pm 0.01\%$ ,  $0.04 \pm 0.03\%$ , and  $0.03 \pm 0.02\%$ . When the last nucleotide of the PAM sequence was T, the survival rates of cells with crRNAs targeting *crtYef* were  $0.02 \pm 0.005\%$ ,  $65.7 \pm 21.77\%$ ,  $91.17 \pm 11.62\%$ ,  $23.28 \pm 12.35\%$ ,  $0.02 \pm 0.02\%$ , and  $13.98 \pm 3.25\%$ . When the last nucleotide of the PAM sequence was C, G, or A, the survival rates of cells with crRNAs targeting *crtYef* were  $0.16 \pm 0.19\%$ ,  $0.007 \pm 0.005\%$ ,  $0.014 \pm 0.008\%$ ,  $50.06 \pm 17.05\%$ ,  $0.01 \pm 0.007\%$ , and  $0.007 \pm 0.005\%$  (Fig. 2b, c). These results showed that when the last nucleotide of PAM was T, the efficiencies of that crRNA were the lowest compared with other corresponding nucleotides. This was consistent with previous studies in human cells [35]. Therefore, we avoided using T as the last nucleotide of the PAM sequence. Furthermore, the highest efficiencies were observed for crRNAs when the last PAM sequence nucleotide was A or C. Therefore, subsequent experiments were carried out using the PAM sequences with A or C as the last nucleotide.

We then tested the role of the second nucleotide of the PAM sequence. We designed, assembled, and tested crRNAs with 5'-XCTA/C-3', 5'-XGTA/C-3', 5'-XATA/C-3', and 5'-XTTA-3' PAM sequences. The survival rates of cells with the 5'-XCTA/C-3' PAM sequence targeting *upp* were  $0.29 \pm 0.0001\%$ ,  $94.42 \pm 0.02\%$ , and  $93.37 \pm 0.05\%$  and targeting *crtYef* were  $89.86 \pm 0.09\%$ ,  $0.03 \pm 0.0002\%$ , and  $66.05 \pm 0.08\%$ . The survival rates of cells with the 5'-XGTA/C-3' PAM sequence targeting *upp* were  $97.51 \pm 0.02\%$ ,  $89.81 \pm 0.09\%$ , and  $98.21 \pm 0.02\%$  and targeting *crtYef* were  $94.7 \pm 0.03\%$ ,  $97.69 \pm 0.02\%$ , and  $96.84 \pm 0.01\%$ . The survival rates of cells with the 5'-XATA/C-3' PAM sequence targeting *upp* were  $98.59 \pm 0.004\%$ ,  $97.69 \pm 0.02\%$ , and  $66.62 \pm 0.2\%$  and targeting *crtYef* were  $99.11 \pm 0.008\%$ ,  $96.84 \pm 0.02\%$ , and  $96.84 \pm 0.01\%$ . The

survival rates of cells with the 5'-XTTA-3' PAM sequence targeting *upp* were  $0.01 \pm 0.0008\%$ ,  $0.07 \pm 0.002\%$ , and  $0.02 \pm 0.001\%$  and targeting *crtYef* were  $0.01 \pm 0.0003\%$ ,  $0.02 \pm 0.0006\%$ , and  $0.2 \pm 0.0004\%$ . Meanwhile, the survival rate of control cells was  $100 \pm 13.48\%$  (Fig. 2d, e). These results showed that when T or C was the second nucleotide in the PAM sequence, the crRNA had a relatively high efficiency.

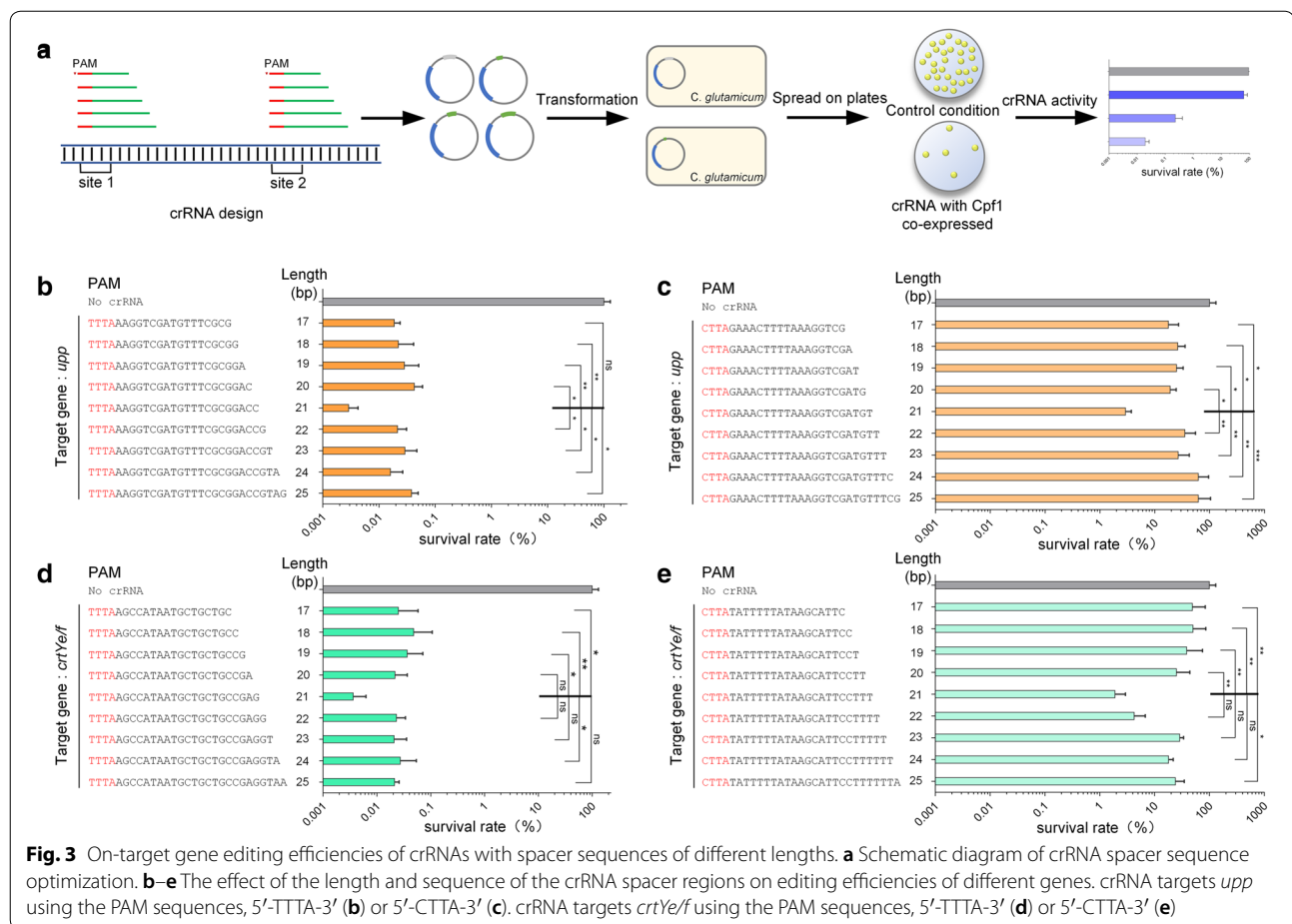
We next sought to test the effect of changing the first nucleotide using the PAM sequences, 5'-CTTA-3', 5'-GTTA-3', 5'-ATT A-3', and 5'-TTTA-3' (Fig. 2f, g). When the first nucleotide of the PAM sequence was T, the survival rates of cells with crRNAs were as low as  $0.032 \pm 0.007\%$ ,  $0.030 \pm 0.01\%$ ,  $0.038 \pm 0.01\%$ ,  $0.014 \pm 0.002\%$ ,  $0.015 \pm 0.002\%$ , and  $0.031 \pm 0.008\%$ , indicating that the crRNA containing the PAM sequence, 5'-TTTA-3', had the highest targeting efficiency. When the first nucleotide of the PAM sequence was C, the survival rates of cells with crRNAs were  $94.06 \pm 5.84\%$ ,  $73.10 \pm 6.68\%$ , and  $96.78 \pm 4.23\%$ , indicating that the crRNA had a low targeting efficiency when the PAM sequence was 5'-CTTA-3'.

Taken together, these data clearly showed that FnCpf1 required a PAM sequence defined as 5'-NYTV-3', where N represents any nucleotide, Y represents T or C, and V represents A, C, or G. Among these sequences, 5'-TTTA/C-3' was the preferred design.

### The effect of spacer sequence length on Cpf1-mediated genome editing

To determine the optimal length of the crRNA spacer sequence, 18 crRNAs targeting *C. glutamicum upp* and *crtYef* genes were constructed with 17–25 bp spacers (Fig. 3). A series of crRNAs, that could be functional in the presence of the preferred 5'-TTTA-3' PAM sequence, were designed to cleave *upp* or *crtYef*. As shown in Fig. 3b, the survival rate of cells with the crRNA targeting *upp* was  $0.003 \pm 0.001\%$  when the spacer length was 21 bp, while survival rates of cells with other crRNAs containing 17–20 bp or 22–25 bp spacer sequences were 0.016–0.042%. Similarly, the survival rate of cells with the crRNA targeting *crtYef* was  $0.003 \pm 0.002\%$ , when the spacer length was 21 bp, while survival rates of cells with other crRNAs containing 17–20 bp or 22–25 bp spacer sequences were 0.021–0.048% (Fig. 3d).

To further confirm the effect of spacer sequence length on targeting efficiency, a series of crRNAs that could be functional in the presence of the relatively low-efficient 5'-CTTA-3' PAM sequence, were designed to cleave *upp* or *crtYef*. The survival rate of cells with the *upp*-targeting crRNA containing a 21 bp spacer sequence was  $2.91 \pm 0.66\%$ , while the survival rates of cells with other crRNAs



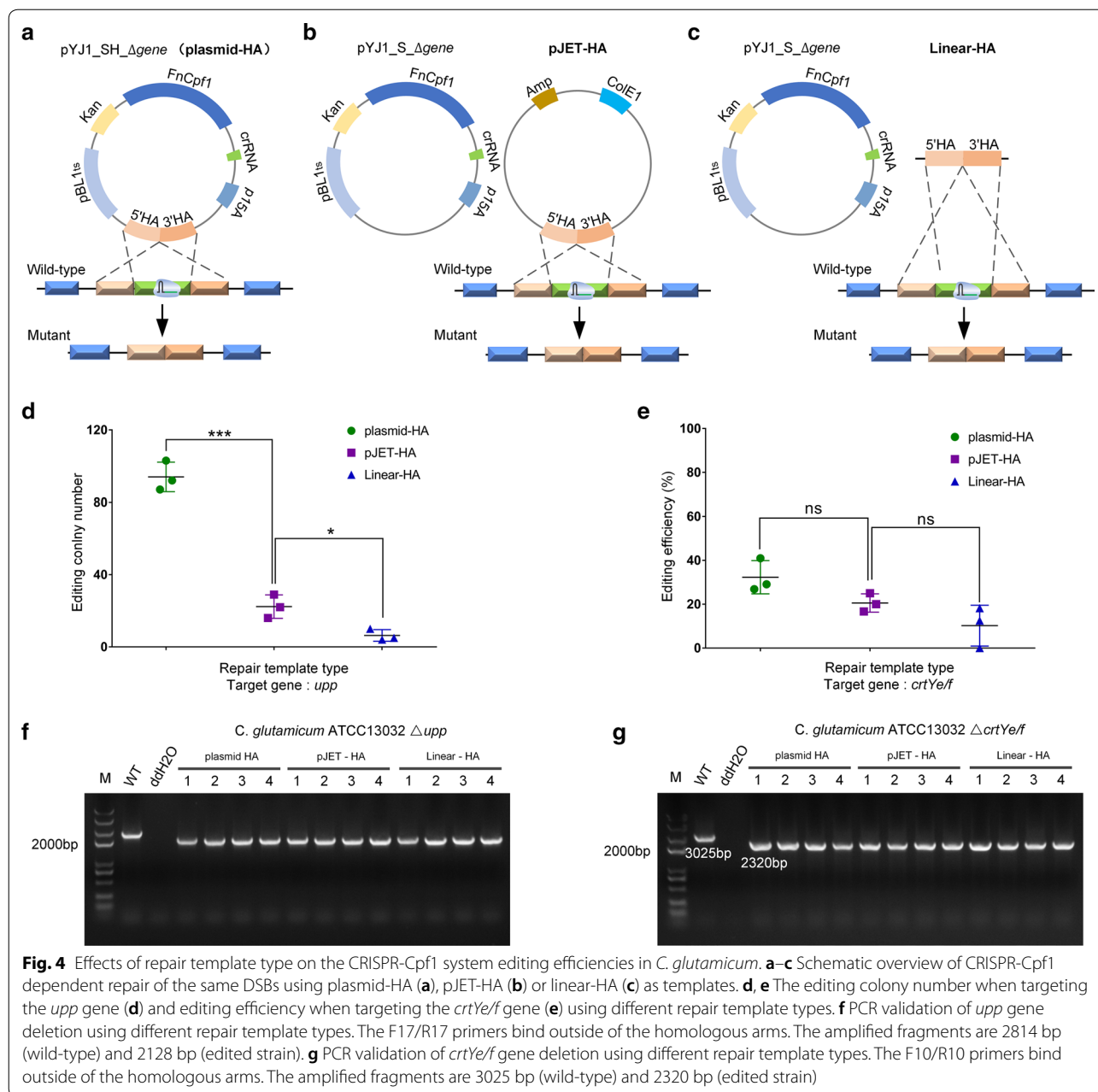
containing 17–20 bp or 22–25 bp spacer sequences were much higher, ranging from 17.75 to 62.37% (Fig. 3c). Similarly, the survival rate of cells with the crRNA containing a 21 bp spacer sequence targeting *crtYef* was  $1.89 \pm 0.85\%$ , while the survival rates of cells with the other crRNAs containing 17–20 bp or 22–25 bp spacer sequences ranged from 4.23 to 50.07% (Fig. 3e). These results showed that a 21 bp spacer sequence had the highest efficiency for gene editing using FnCpf1.

#### The effect of repair template type on Cpf1-mediated genome editing

A DSB induced by CRISPR-Cpf1 in vivo can be repaired through HR in the presence of a plasmid-borne template [21, 36, 37]. In this study, we investigated whether another type of DNA could be used as a repair template. Two target genes, *upp* and *crtYef*, were chosen because *C. glutamicum* cells would undergo an obvious phenotype change if any of these two genes were deleted. Different repair templates were used to determine their effect on editing efficiencies. When *upp* was edited, the colonies became resistant to 5-FU and when *crtYef* was

edited, the colonies turned red. The editing efficiency could be calculated by dividing the number of edited single colonies on the selection plate by the total number of colonies on the control plate.

The types of DNA tested in our study were plasmid-HA, pJET-HA and linear-HA. The repair template was first ligated into the pYJ1\_S\_Δgene vector, which has a replicon of *C. glutamicum* (Fig. 4a) and the pJET blunt vector, which cannot replicate in *C. glutamicum* (Fig. 4b). The linearized donor was then used to determine whether it was applicable in *C. glutamicum* (Fig. 4c). The number of *upp*-edited colonies when using the linear-HA template was  $6.73 \pm 0.02\%$  of the number when using the plasmid-HA template. The average number of colonies with the plasmid-HA, pJET-HA, and linear-HA templates was  $94 \pm 6.68$ ,  $22 \pm 5.31$ , and  $6 \pm 2.62$ , respectively (Fig. 4d). Further, we assessed the effect of different repair templates on *crtYef*-editing efficiency. When using plasmid-HA, pJET-HA, and linear-HA templates, the *crtYef*-editing efficiencies were  $32.30 \pm 6.18\%$ ,  $20.56 \pm 3.42\%$ , and  $10.23 \pm 7.59\%$ , respectively (Fig. 4e). The same gene knockout efficiencies were obtained with

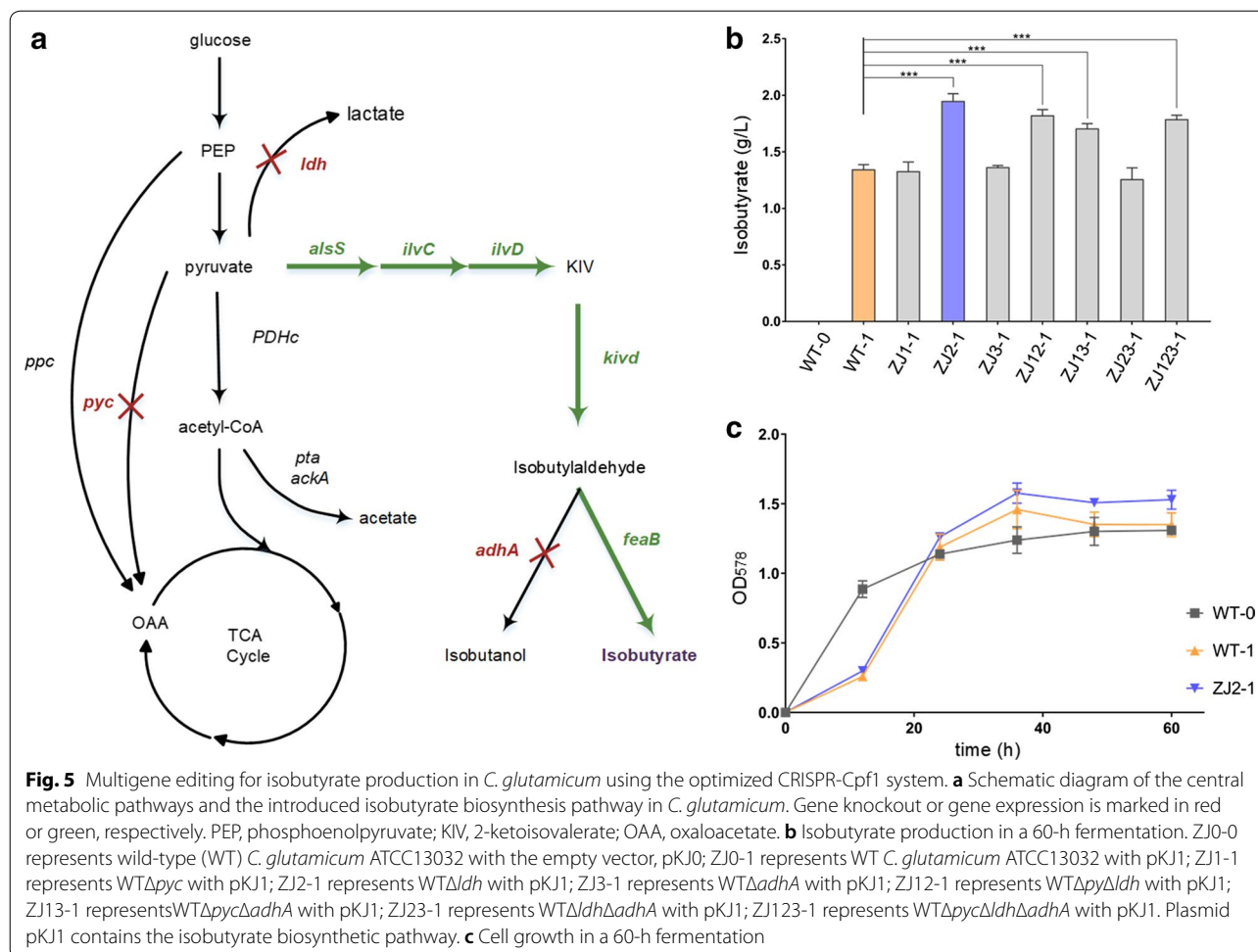


in vitro linearized DNA obtained by either PCR-amplification or restriction-enzyme digestion of the donor plasmid (data not shown). These results showed that the plasmid-HA template gave the highest gene editing efficiency and the pJET-HA template gave an intermediate level of efficiency.

#### Application of the CRISPR-Cpf1 method to modify multiple genes for microbial production of isobutyrate

Our CRISPR-Cpf1 mediated genome editing procedure significantly enhanced the ability to iteratively introduce

well-designed genomic mutations in *C. glutamicum*. To illustrate its potential application in metabolic engineering, we used our system to modify *C. glutamicum* for the production of isobutyrate. We applied a strategy of over-expressing the 2-keto acid biosynthesis pathway (Fig. 5), which has also been engineered into *Escherichia coli*. The yield of isobutyrate in engineered *E. coli* has been reported to be approximately 4.8 g/L [38]. The 2-keto acid biosynthesis pathway includes *alsS* (*Bacillus subtilis*) and *ilvCD* (*C. glutamicum*), along with downstream genes for the subsequent decarboxylation (*kivD* from



*Lactococcus lactis*) and oxidation (*feaB* from *E. coli*) of 2-ketoisovalerate to isobutyrate. The expression of these five genes was driven by the strong constitutive promoter, *Peftu*, in the plasmid, pKJ1. The empty vector, pKJ0, was used as a negative control.

The wild-type (WT) strain *C. glutamicum* with pKJ1 (WT-1) produced  $1.34 \pm 0.03$  g/L of isobutyrate in 60 h (Fig. 5b). We then attempted to increase isobutyrate production by using the CRISPR-Cpf1 system to inactivate several enzymes that may consume precursors of the isobutyrate pathway. The genes, *pyc* (encoding pyruvate carboxylase), *ldh* (encoding lactate dehydrogenase), and *adhA* (encoding alcohol dehydrogenase) were chosen to block the competitive pathways (Fig. 5a). We constructed three single-knockout strains, named ZJ1, ZJ2, ZJ3; three double-knockout strains, named ZJ12, ZJ13, ZJ23; and one triple-knockout strain, named ZJ123 (Table 1). The  $\Delta$ *pyc* and  $\Delta$ *adhA* knockout strains (ZJ1 and ZJ3) and the  $\Delta$ *ldh* $\Delta$ *adhA* strain (ZJ23) did not show increased isobutyrate production compared with the WT strain. By contrast, isobutyrate production in the  $\Delta$ *ldh* strain (ZJ2)

increased to  $2.01 \pm 0.05$  g/L (Fig. 5b), while the  $\Delta$ *pyc* $\Delta$ *ldh* (ZJ12),  $\Delta$ *pyc* $\Delta$ *adhA* (ZJ13), and  $\Delta$ *pyc* $\Delta$ *ldh* $\Delta$ *adhA* (ZJ123) strains, containing pKJ1, produced  $1.82 \pm 0.04$ ,  $1.70 \pm 0.03$ , and  $1.78 \pm 0.03$  g/L of isobutyrate, respectively. Interestingly, the isobutyrate-producing strains also reached a higher cell density than the control strain (Fig. 5c).

## Discussion

Recently, CRISPR-Cpf1 was investigated as a leading-edge tool for genome editing in many bacteria. It was reported to be suitable for *C. glutamicum*, but the efficiency of gene editing was  $\sim 15\%$  when targeting a 705 bp gene [12]. Effective gene editing requires the formation of a functional complex between Cpf1, crRNA, and the target DNA strand. In this study, we systematically investigated various parameters of a *C. glutamicum* CRISPR-Cpf1 system, including the PAM sequence, the length of the spacer sequence, and the type of repair template.

FnCpf1 requires only a single crRNA, without a tracrRNA, and it recognizes thymine-rich PAM sequences.



**Table 1 Strains and plasmids used in this study**

Strain or plasmid	Description <sup>a</sup>	Reference or source
Strain		
<i>E. coli</i> Top10	General cloning host	Biomed
<i>C. glutamicum</i> ATCC 13032	Wild-type strain	ATCC
<i>C. glutamicum</i> $\Delta upp$	ATCC 13032 derivative with its <i>upp</i> gene deleted	This study
<i>C. glutamicum</i> $\Delta crtYe/f$	ATCC 13032 derivative with its <i>crtYe/f</i> gene deleted	This study
ZJ1	ATCC 13032 derivative with its <i>pyc</i> gene deleted	This study
ZJ2	ATCC 13032 derivative with its <i>ldh</i> gene deleted	This study
ZJ3	ATCC 13032 derivative with its <i>adhA</i> gene deleted	This study
ZJ12	ATCC 13032 derivative with its <i>pyc</i> gene and <i>ldh</i> gene deleted	This study
ZJ13	ATCC 13032 derivative with its <i>pyc</i> gene and <i>adhA</i> gene deleted	This study
ZJ23	ATCC 13032 derivative with its <i>ldh</i> gene and <i>adhA</i> gene deleted	This study
ZJ123	ATCC 13032 derivative with its <i>pyc</i> gene, <i>ldh</i> gene and <i>adhA</i> gene deleted	This study
WT-0	<i>C. glutamicum</i> ATCC 13032 + pKJ0	This study
WT-1	<i>C. glutamicum</i> ATCC 13032 + pKJ1	This study
ZJ1-1	ZJ1 + pKJ1	This study
ZJ2-1	ZJ2 + pKJ1	This study
ZJ3-1	ZJ3 + pKJ1	This study
ZJ12-1	ZJ12 + pKJ1	This study
ZJ13-1	ZJ13 + pKJ1	This study
ZJ23-1	ZJ23 + pKJ1	This study
ZJ123-1	ZJ123 + pKJ1	This study
Plasmid <sup>b</sup>		
pJYS3_ $\Delta crtYf$	pBL1 <sup>ts</sup> ori V <i>C. glutamicum</i> , Kan <sup>R</sup> pSC101 ori V <i>E. coli</i> PlacM-FnCpf1, Pj23119-crRNA targeting <i>crtYf</i> , 1 kb upstream and downstream homologous arms flanking the 705 bp deletion fragment inside <i>crtYf</i>	Jiang et al. [12]
pYJ1	pBL1 <sup>ts</sup> ori V <i>C. glutamicum</i> , Kan <sup>R</sup> p15A ori V <i>E. coli</i> PlacM-FnCpf1, crRNA expression cassette	This study
pYJ1_S_ $\Delta upp$	pYJ1 carrying spacer sequence targeting <i>upp</i> gene	This study
pYJ1_SH_ $\Delta upp$	pYJ1_S_ $\Delta upp$ carrying upstream and downstream homologous arm targeting <i>upp</i> gene	This study
pYJ1_S_ $\Delta crtYe/f$	pYJ1 carrying spacer sequence targeting <i>crtYe/f</i> gene	This study
pYJ1_SH_ $\Delta crtYe/f$	pYJ1_S_ $\Delta crtYe/f$ carrying upstream and downstream homologous arm targeting <i>crtYe/f</i> gene	This study
pYJ1_S_ $\Delta pyc$	pYJ1 carrying spacer sequence targeting <i>pyc</i> gene	This study
pYJ1_SH_ $\Delta pyc$	pYJ1 carrying spacer sequence and homologous arm targeting <i>pyc</i> gene	This study
pYJ1_S_ $\Delta ldh$	pYJ1 carrying spacer sequence targeting <i>ldh</i> gene	This study
pYJ1_SH_ $\Delta ldh$	pYJ1 carrying spacer sequence and homologous arm targeting <i>ldh</i> gene	This study
pYJ1_S_ $\Delta adhA$	pYJ1 carrying spacer sequence targeting <i>adhA</i> gene	This study
pYJ1_SH_ $\Delta adhA$	pYJ1 carrying spacer sequence and homologous arm targeting <i>adhA</i> gene	This study
pJET_HA_ $\Delta upp$	pJET vector carrying upstream and downstream homologous arm targeting <i>upp</i> gene	This study
pJET_HA_ $\Delta crtYe/f$	pJET vector carrying upstream and downstream homologous arm targeting <i>crtYe/f</i> gene	This study
pKS167	NG2 ori; Kan <sup>R</sup> ; Pefu:: <i>alsS-ilvCD-kivd-adhA</i>	Smith et al. [44]
pKJ0	NG2 ori; Kan <sup>R</sup> ; Pefu	This study
pKJ1	NG2 ori; Kan <sup>R</sup> ; Pefu:: <i>alsS-ilvCD-kivd-feaB</i>	This study

<sup>a</sup> Kan<sup>R</sup> represents resistance to kanamycin

<sup>b</sup> crRNA expression plasmids with changed spacer sequences are not listed here. A full list of spacer sequences used in this study is shown in Additional file 1: Table S2

The PAM sequence is a key sequence regulating the accurate binding of crRNA to the genome. FnCpf1 may recognize the PAM sequence via shape- and base-readout mechanisms [40]. The PAM-binding channel of Cpf1 has conformational flexibility, which allows the recognition

of different PAM sequences. However, the optimal PAM sequence for the manipulation of *C. glutamicum* has not yet been reported.

Therefore, we constructed a lethal reporter system and used it to examine the PAM sequence preference

of CRISPR-Cpf1 in *C. glutamicum*. Using two different target genes, T was found to be preferred at the first nucleotide position, although all nucleotides were functional at this position. T or C was the preferred at the second nucleotide position. At the third nucleotide of the PAM sequence, T is generally believed to optimal [25] and therefore, we did not test an alternative nucleotide at this position. When the last nucleotide of the PAM sequence was T, the efficiency of the crRNA was the lowest compared with other nucleotides at this position, which agreed with the results reported by Tu et al. [35]. However, crRNA had the highest efficiency of cutting target sites within the *upp* and *crtYe/f* genes when the last nucleotide of the PAM sequence was A or C. Based on these results, we concluded that the PAM sequence, 5'-NYTV-3' (N=T/A/G/C, Y=T/C, V=A/C/G) was preferred for FnCpf1 to achieve a high targeting efficiency in the *C. glutamicum* genome. These results shed light on the PAM sequence requirements of FnCpf1 and the molecular basis of PAM recognition in *C. glutamicum*.

We further investigated the effect of different crRNA spacer sequence lengths on the efficiency of Cpf1-dependent editing. We found that FnCpf1 had the highest activity in *C. glutamicum* when a 21 bp crRNA spacer sequence was used. Structural studies have shown that only a 20 bp RNA–DNA heteroduplex is formed between the target DNA strand and a 24 bp crRNA spacer sequence [41, 42]. It was speculated that a 21 bp spacer sequence may form a complex with its target DNA strand and FnCpf1 in human cells, in which FnCpf1 has improved activity and higher fidelity [35]. This was an unexpected result which requires further investigation. When we attempted to cleave another target DNA sequence within the *upp* gene using the 5'-TTTC-3' PAM sequence, a 20 bp crRNA spacer sequence (5'-cgt-gcagcagccaacgacct) completely lost its activity, whereas other crRNAs with 17–19 bp or 21–25 bp spacer sequences showed high activity (data not shown).

If the plasmids containing the crRNA and template could be constructed independently, the speed of genome editing would be accelerated. We attempted to introduce the repair template into the pJET vector, which cannot replicate and therefore, introduces a lower metabolic burden on the host. Although the repair efficiency of pJET derivatives was not as high as that of replicable plasmid-borne templates, it was sufficient for gene editing. Finally, we assessed whether a linear repair template could be used in *C. glutamicum*. For the first time, we showed that a linear repair template could be successfully utilized to edit genomic DNA in *C. glutamicum*. However, the editing efficiency was relatively low, likely because a restriction repair system may have degraded the linear repair template prior to the genome repair process.

*C. glutamicum* is an important amino acid production strain and is highly suitable for the production of isobutyrate, which is an acid with high market demand. Here, we introduced an isobutyrate synthesis pathway into *C. glutamicum* and confirmed that the transgenic strain produced isobutyrate successfully, albeit at low rates. To further engineer a potential industrial isobutyrate production strain, we used our genome editing system to knock out the *pyc*, *ldh*, and *adhA* genes from the genome of *C. glutamicum*. Among all the host strains we constructed, the  $\Delta ldh$  strain, ZJ2, containing pKJ1 produced the highest yield of isobutyrate. Knocking out *ldh* blocks the production of acetic acid, which increases the pyruvate pool available for isobutyrate production. However, *pyc* knockout did not significantly increase isobutyrate production in *C. glutamicum*, probably due to a reduction in the supply of oxaloacetate in the citric acid cycle, resulting in unbalanced redox levels. Similarly, *adhA* knockout did not significantly increase isobutyrate production, indicating that other enzymes with alcohol dehydrogenase activity may also be present in *C. glutamicum*. The same changes in the host genome were previously successfully introduced into *E. coli* [38, 39], but except the knockout of *ldh*, the knockout of *pyc* and *adhA* didn't work efficiently in *C. glutamicum*. The metabolic engineering of production hosts requires multiple rounds of genome editing to optimize production. The high efficiency of the crRNA in our study helps avoid the additional workload due to false positives caused by poor crRNA design. Using linear-HA or pJET-HA can decrease the time required for plasmid construction and can potentially facilitate multiplex gene editing when constructing engineered *C. glutamicum*.

## Conclusions

In summary, we have comprehensively and quantitatively assessed the effects of PAM sequence, spacer sequence length, and repair template type on the efficiency of the CRISPR-Cpf1 system in *C. glutamicum*. Our study offers insights into FnCpf1 endonuclease function and Cpf1-based genome editing.

## Methods

### Strains and culture conditions

All bacterial strains used in this work are listed in Table 1. The Top10 *E. coli* strain was used for routine cloning procedures. *C. glutamicum* ATCC13032 was used as the parent strain for genetic modifications. All engineered strains were transformed by electroporation. All strains were kept at  $-80^{\circ}\text{C}$  as glycerol stocks prepared in Luria-Bertani (LB) or BHIS broth containing 15% glycerol.

*E. coli* Top10 was grown aerobically in LB medium (10 g/L tryptone, 5 g/L yeast extract, and 10 g/L NaCl)

at 37 °C, with shaking at 200 rpm. *C. glutamicum* ATCC 13032 strains were routinely cultivated in BHIS medium (37 g/L brain heart infusion medium and 91 g/L sorbitol) at 30 °C, with shaking at 200 rpm. Antibiotics were added at the following concentrations: 50 µg/mL kanamycin, 100 µg/mL ampicillin, and 25 µg/mL chloramphenicol for *E. coli* and 25 µg/mL kanamycin and 10 µg/mL chloramphenicol for *C. glutamicum*. Colonies with successful knockout of *upp* were selected on plates of CGXII medium (20 g/L  $[\text{NH}_4]_2\text{SO}_4$ , 5 g/L urea, 1 g/L  $\text{KH}_2\text{PO}_4$ , 1 g/L  $\text{K}_2\text{HPO}_4$ , 0.25 g/L  $\text{MgSO}_4 \cdot 7\text{H}_2\text{O}$ , 10 mg/L  $\text{CaCl}_2$ , 10 mg/L  $\text{FeSO}_4 \cdot 7\text{H}_2\text{O}$ , 10 mg/L  $\text{MnSO}_4 \cdot \text{H}_2\text{O}$ , 1 mg/L  $\text{ZnSO}_4 \cdot 7\text{H}_2\text{O}$ , 0.2 mg/L  $\text{CuSO}_4 \cdot 5\text{H}_2\text{O}$ , 0.02 mg/L  $\text{NiCl}_2 \cdot 6\text{H}_2\text{O}$ , 0.2 mg/L biotin, 42 g/L 3-morpholinopropanesulfonic acid [MOPS], and 40 g/L glucose), containing 100 µM 5-FU (from a 100 mM stock in dimethyl sulfoxide). *C. glutamicum* fermentations were also performed in CGXII medium.

### Plasmid constructions

All plasmids used in this study are listed in Table 1. The sequences of the primers, crRNAs, and oligonucleotides are listed in Additional file 1: Tables S1 and S2. Plasmids and genomic DNA were extracted using the TIANamp Mini Plasmid Kit (TIANGEN BIOTECH, Beijing, China) and TIANamp Bacteria DNA Kit (TIANGEN BIOTECH), according to the manufacturer's instructions. PCR was performed using TransStart FastPfu Fly DNA Polymerase (TransGen Biotech, Beijing, China). DNA was extracted from agarose gels using the HiPure Gel Pure DNA Micro Kit (Magen, Guangzhou, China). Cloning was performed using commercially available restriction endonucleases, T4 DNA ligase, the CloneJET PCR Cloning Kit (Thermo Scientific, Waltham, MA, USA), and the Gibson assembly method [43].

The plasmid, pYJ1, was constructed via Gibson assembly using the following three DNA fragments: a Cpf1 expression cassette with a temperature-sensitive replicon; pBL<sup>ts</sup> with a kanamycin resistance gene fragment, originally constructed by Jiang et al. [12]; a *E. coli* replicon p15A and a crRNA expression cassette. The plasmid, pJYS3\_Δ*crtYf* [12], was used as a template to amplify the fragment using F1/R1 primers and an *ApaI* restriction enzyme cutting site was added to the primers to insert homologous arms. The crRNA expression cassette consisted of the constitutive promoter, pJ23119; a 19 bp direct repeat sequence of the crRNA; a 25 bp sequence with an *AarI* restriction enzyme site to insert the spacer sequence, and an *rrnB* terminator. The nucleotide sequences of the crRNA expression cassettes used in this study are listed in Additional file 1: Table S3. To generate pYJ1\_S\_Δgene, pYJ1 was linearized with *AarI* and a pair of primers (such as F4/R4) was annealed to

form a dsDNA fragment with cohesive ends, which was then ligated to pYJ1 using T4 DNA ligase. To generate pYJ1\_SH\_Δgene, pYJ1\_S\_Δgene was linearized with *ApaI*. The *C. glutamicum* ATCC13032 genome was used as a template to amplify 500 bp upstream and downstream homologous arms using corresponding primers (such as F5/R5 and F6/R6, respectively). The *ApaI* restriction enzyme site was introduced by the primers and the two fragments were assembled via another round of PCR. The purified PCR product was then cut using *ApaI* and inserted into the linearized pYJ1\_S\_Δgene plasmid. To construct pJET\_HA\_Δgene, homologous arms were amplified using the primer pairs like F15/R15 and the PCR products were ligated to the vector, pJET1.2 (CloneJET PCR Cloning Kit, Thermo Fisher Scientific). To construct the plasmid, pKJ0, the backbone of pKS167 was amplified using the primer pair, F33/R33 [44] and the PCR product was used directly to transform competent *E. coli* cells. The plasmid was verified by PCR and sequencing. To construct the plasmid, pKJ1, the backbone of pKS167 was amplified using the primer pair, F35/R35. The *feaB* gene was amplified from the *E. coli* genome using the primer pair, F36/R36. The two fragments were then assembled using the Gibson assembly method.

### Iterative genome editing procedure

Electrocompetent cells were generated as described previously [45]. In the plasmid-borne template system, 500 ng of pYJ1\_S\_Δgene or pYJ1\_SH\_Δgene was used for each electroporation. For the linear-HA and pJET-HA templates, 500 ng of pYJ1\_S\_Δgene and 1 µg of the repair template were mixed together to co-transform competent cells. Electroporation was performed using a Gene Pulser system (Bio-Rad, Hercules, CA, USA) set to 25 µF, 1.25 kV/cm, and 200Ω. Following exposure to a single electric pulse, the cell suspension was immediately transferred into 1 mL of pre-warmed (46 °C) BHIS medium and incubated for 6 min at 46 °C without shaking. Subsequently, *C. glutamicum* cells were incubated with shaking at 200 rpm for 2 h at 30 °C. Finally, cells were spread on selective BHIS agar plates containing 25 µg/mL kanamycin. Transformants were confirmed by PCR amplification.

For plasmid curing, colonies were seeded into BHIS without antibiotics and cultivated for 6–8 h or overnight at 37 °C. To save time, the colonies were then simultaneously inoculated for plasmid curing to allow iterative engineering. After plasmid curing, the cultures were streaked and the colonies were tested for kanamycin sensitivity. The edited colony was then grown to mid-log phase to prepare electrocompetent cells for the next round of editing.

To verify these editing events by Sanger sequencing, colonies were picked and the target region was amplified by PCR. The primers used for PCR amplification and sequencing are listed in Additional file 1: Table S1.

### Determining crRNA targeting efficiency by measuring Cpf1-induced lethality

Plasmids carrying the crRNA expression cassette were introduced into competent cells (500 ng plasmid/100  $\mu$ L of competent cells). After transformation, cells were incubated in BHIS medium for 1 h at 30 °C for recovery. The culture was then streaked on BHIS agar plates containing kanamycin. The colonies were counted after 36–48 h of cultivation and the survival rates for each crRNA were calculated by counting the colonies that formed. To minimize the impact of differences in electroporation efficiency during the preparation of competent cells, the survival rates were further normalized by determining the colony number after transformation with a negative control crRNA plasmid. All transformations were performed in triplicate. The survival rate was calculated according to the following formula:

$$\text{Survival rate} = \left( \frac{[\text{read count}]_{\text{selective}}}{\text{average}[\text{read count}]_{\text{control}}} \right) \times 100\%.$$

### Shake-flask fermentation

Five milliliters of BHIS medium was inoculated with a single colony of the desired *C. glutamicum* strain from a fresh BHIS agar plate and the culture was incubated on a rotary shaker at 30 °C overnight. For isobutyrate production, 200  $\mu$ L of the overnight culture was transferred into a 250-mL anaerobic shake flask with 20 mL of CGXII medium, containing 40 g/L glucose. Fermentation was performed at 30 °C, with shaking at 200 rpm. Samples were drawn every 12 h to determine metabolite concentrations and perform OD<sub>578</sub> measurements. All experiments were performed in at least three biological replicates.

### Metabolic analysis

Organic acids in the culture supernatants were quantified using an Agilent 1260 Infinity HPLC system, equipped with an RID detector and an Aminex HPX-87H cation exchange column (BioRad). The samples were first filtered through a 0.22- $\mu$ m filter, then loaded onto the column operated at 60 °C, eluted with 5 mM H<sub>2</sub>SO<sub>4</sub> at a flow rate of 0.5 mL/min, and detected via refractive index. The data are presented as mean values, with error bars indicating standard deviation.

## Additional file

**Additional file 1.** Additional Figures S1, S2 and Tables S1–S3.

### Abbreviations

CRISPR: clustered regularly interspaced short palindromic repeats; FnCpf1: Cpf1 derived from *F. novicida* (NC\_008601); crRNA: CRISPR RNA; tracrRNA: trans-activating CRISPR RNA; PAM: protospacer adjacent motif; DSBs: double-strand breaks; dsDNA: double strand DNA; HR: homologous recombination; OD<sub>578</sub>: optical density at 578 nm; HPLC: high-pressure liquid chromatography detector; RID: refractive index detector; Kan: kanamycin; PCR: polymerase chain reaction; 5-FU: 5-fluorouracil; PEP: phosphoenolpyruvate; KIV: 2-ketoisovalerate; OAA: oxaloacetate.

### Authors' contributions

JZ, FY and YH conceived this study, designed and conducted the experiments. JZ, FY and YY performed the experiments. JZ, FY, YJ and YH analyzed the data, JZ, FY and YH wrote the manuscript. All authors read and approved the final manuscript.

### Author details

<sup>1</sup> Key Laboratory of Molecular Medicine and Biotherapy, School of Life Sciences, Beijing Institute of Technology, No. 5 South Zhongguancun Street, Beijing 100081, China. <sup>2</sup> UCLA Institute of Advancement (Suzhou), 10 Yueliangwan Road, Suzhou Industrial Park, Suzhou 215123, China. <sup>3</sup> Key Laboratory of Synthetic Biology, Institute of Plant Physiology and Ecology, Shanghai Institutes for Biological Sciences, Chinese Academy of Sciences, Shanghai 200032, China.

### Acknowledgements

The authors wish to thank Beijing Institute of Technology for the supply of microplate reader (BioTek Cytation 3).

### Competing interests

The authors declare that they have no competing interests.

### Availability of data and materials

All data generated or analyzed during this study are included in this published article and its additional files. The authors are willing to provide any additional data and materials related to this research that may be requested for research purposes.

### Consent for publication

Not applicable.

### Ethics approval and consent to participate

Not applicable.

### Funding

The author would like to acknowledge financial support of the National Natural Science Foundation of China (Grant No. 2167026), the National Key Research and Development Plan (Grant No. 2017YFD0201400), and Fundamental Research Funds for the Central Universities.

### Publisher's Note

Springer Nature remains neutral with regard to jurisdictional claims in published maps and institutional affiliations.

Received: 17 October 2018 Accepted: 19 March 2019

Published online: 25 March 2019

### References

- Shin KC, Sim DH, Seo MJ et al. Increased production of food-grade d-tagatose from d-Galactose by permeabilized and immobilized cells of *Corynebacterium glutamicum*, a GRAS Host, expressing d-Galactose



- Isomerase from *geobacillus thermodenitrificans*. *J Agric Food Chem*. 2016;64(43):8146–53.
2. Srivastava P, Deb JK. Gene expression systems in corynebacteria. *Protein Expr Purif*. 2005;40(2):221–9.
  3. Blombach B, Seibold GM. Carbohydrate metabolism in *Corynebacterium glutamicum* and applications for the metabolic engineering of L-lysine production strains. *Appl Microbiol Biotechnol*. 2010;86(5):1313–22.
  4. Hou X, et al. L-Valine production with minimization of by-products' synthesis in *Corynebacterium glutamicum* and *Brevibacterium flavum*. *Amino Acids*. 2012;43(6):2301–11.
  5. Mckinlay JB, Vieille C, Zeikus JG. Prospects for a bio-based succinate industry. *Appl Microbiol Biotechnol*. 2007;76(4):727–40.
  6. Siebert D, Wendisch VF. Metabolic pathway engineering for production of 1,2-propanediol and 1-propanol by *Corynebacterium glutamicum*. *Biotechnol Biofuels*. 2015;8(1):1–13.
  7. Song Y, et al. Engineered *Corynebacterium glutamicum* as an endotoxin-free platform strain for lactate-based polyester production. *Appl Microbiol Biotechnol*. 2012;93(5):1917–25.
  8. Schäfer A, et al. Small mobilizable multi-purpose cloning vectors derived from the *Escherichia coli* plasmids pK18 and pK19: selection of defined deletions in the chromosome of *Corynebacterium glutamicum*. *Gene*. 1994;145(1):69.
  9. Hu J, et al. Construction and application of an efficient multiple-gene-deletion system in *Corynebacterium glutamicum*. *Plasmid*. 2013;70(3):303–13.
  10. Ma W, et al. Development of a markerless gene replacement system in *Corynebacterium glutamicum* using upp as a counter-selection marker. *Biotech Lett*. 2015;37(3):609–17.
  11. Suzuki N, et al. New multiple-deletion method for the *Corynebacterium glutamicum* genome, using a mutant lox sequence. *Appl Environ Microbiol*. 2005;71(12):8472–80.
  12. Yu J, et al. CRISPR-Cpf1 assisted genome editing of *Corynebacterium glutamicum*. *Nat Commun*. 2017;8:15179.
  13. Shuman S, Glickman MS. Bacterial DNA repair by non-homologous end joining. *Nat Rev Microbiol*. 2007;5(11):852–61.
  14. Jiang W, et al. RNA-guided editing of bacterial genomes using CRISPR-Cas systems. *Nat Biotechnol*. 2013;31(3):233–9.
  15. Li H, et al. CRISPR-Cas9 for the genome engineering of cyanobacteria and succinate production. *Metab Eng*. 2016;38:293–302.
  16. Oh JH, van Pijkeren JP. CRISPR-Cas9-assisted recombinering in *Lactobacillus reuteri*. *Nucleic Acids Res*. 2014;42(17):e131.
  17. Tong Y, et al. CRISPR-Cas9 based engineering of actinomycetal genomes. *ACS Synth Biol*. 2015;4(9):1020.
  18. Xu T, et al. Efficient genome editing in *Clostridium cellulolyticum* via CRISPR-Cas9 nickase. *Appl Environ Microbiol*. 2015;81(13):4423–31.
  19. Garst AD, et al. Genome-wide mapping of mutations at single-nucleotide resolution for protein, metabolic and genome engineering. *Nat Biotechnol*. 2017;35(1):48–55.
  20. Lun C, Bikard D. Consequences of Cas9 cleavage in the chromosome of *Escherichia coli*. *Nucleic Acids Res*. 2016;44(9):4243–51.
  21. Zerbini F, et al. Large scale validation of an efficient CRISPR/Cas-based multi gene editing protocol in *Escherichia coli*. *Microb Cell Fact*. 2017;16(1):68.
  22. Dong D, et al. The crystal structure of Cpf1 in complex with CRISPR RNA. *Nature*. 2016;532(7600):522–6.
  23. Endo A, et al. Efficient targeted mutagenesis of rice and tobacco genomes using Cpf1 from *Francisella novicida*. *Sci Rep*. 2016;6:38169.
  24. Sun B, et al. A CRISPR-Cpf1-assisted non-homologous end joining genome editing system of *Mycobacterium smegmatis*. *Biotechnol J*. 2018;9:e1700588.
  25. Zetsche B, et al. Cpf1 Is a single RNA-guided endonuclease of a class 2 CRISPR-Cas system. *Cell*. 2015;163(3):759–71.
  26. Mojica FJM, Diez-Villasenor C, Garcia-Martinez J, Almendros C. Short motif sequences determine the targets of the prokaryotic CRISPR defence system. *Microbiology*. 2009;155(Pt 3):733–40.
  27. Lei C, et al. The CCTL (Cpf1-assisted Cutting and Taq DNA ligase-assisted Ligation) method for efficient editing of large DNA constructs in vitro. *Nucleic Acids Res*. 2017;45(9):e74.
  28. Tóth E, et al. Cpf1 nucleases demonstrate robust activity to induce DNA modification by exploiting homology directed repair pathways in mammalian cells. *Biol Direct*. 2016;11(1):46.
  29. Cho JS, et al. CRISPR/Cas9-coupled recombinering for metabolic engineering of *Corynebacterium glutamicum*. *Metab Eng*. 2017;42:157–67.
  30. Paix A, Folkmann A, Seydoux G. Precision genome editing using CRISPR-Cas9 and linear repair templates in *C. elegans*. *Methods*. 2017;121–122:86–93.
  31. Yao X, et al. Tild-CRISPR allows for efficient and precise gene knockin in mouse and human cells. *Dev Cell*. 2018;45:526–36.
  32. Krubasik P, Sandmann G. A carotenogenic gene cluster from *Brevibacterium linens* with novel lycopene cyclase genes involved in the synthesis of aromatic carotenoids. *Mol Gen Genet MGG*. 2000;263(3):423–32.
  33. Krubasik P, et al. Detailed biosynthetic pathway to decaprenoxanthin diglucoside in *Corynebacterium glutamicum* and identification of novel intermediates. *Arch Microbiol*. 2001;176(3):217.
  34. Netzer R, et al. Biosynthetic pathway for  $\gamma$ -cyclic sarcinaxanthin in *Micrococcus luteus*: heterologous expression and evidence for diverse and multiple catalytic functions of C(50) carotenoid cyclases. *J Bacteriol*. 2010;192(21):5688.
  35. Tu M, et al. A 'new lease of life': FnCpf1 possesses DNA cleavage activity for genome editing in human cells. *Nucleic Acids Res*. 2017;45(19):11295–304.
  36. Paquet D, et al. Efficient introduction of specific homozygous and heterozygous mutations using CRISPR/Cas9. *Nature*. 2016;533(7601):125.
  37. Richardson CD, et al. Enhancing homology-directed genome editing by catalytically active and inactive CRISPR-Cas9 using asymmetric donor DNA. *Nat Biotechnol*. 2016;34(3):339–44.
  38. Zhang K, et al. A synthetic metabolic pathway for production of the platform chemical isobutyric acid. *ChemSuschem*. 2011;4(8):1068–70.
  39. Xiong M, et al. Improving engineered *Escherichia coli* strains for high-level biosynthesis of isobutyrate. *Aims Energy*. 2015;2(2):60–74.
  40. Yamano T, et al. Structural basis for the canonical and non-canonical PAM recognition by CRISPR-Cpf1. *Mol Cell*. 2017;67(4):633.
  41. Gao P, et al. Type V CRISPR-Cas Cpf1 endonuclease employs a unique mechanism for crRNA-mediated target DNA recognition. *Cell Res*. 2016;26(8):901.
  42. Yamano T, et al. Crystal structure of Cpf1 in complex with guide RNA and target DNA. *Cell*. 2016;165(4):949–62.
  43. Gibson DG, et al. Enzymatic assembly of DNA molecules up to several hundred kilobases. *Nat Methods*. 2009;6(5):343.
  44. Smith KM, Cho KM, Liao JC. Engineering *Corynebacterium glutamicum* for isobutanol production. *Appl Microbiol Biotechnol*. 2010;87(3):1045–55.
  45. Tauch A, et al. Efficient electrotransformation of corynebacterium diphtheriae with a mini-replicon derived from the *Corynebacterium glutamicum* plasmid pGA1. *Curr Microbiol*. 2002;45(5):362–7.

Ready to submit your research? Choose BMC and benefit from:

- fast, convenient online submission
- thorough peer review by experienced researchers in your field
- rapid publication on acceptance
- support for research data, including large and complex data types
- gold Open Access which fosters wider collaboration and increased citations
- maximum visibility for your research: over 100M website views per year

At BMC, research is always in progress.

Learn more [biomedcentral.com/submissions](https://biomedcentral.com/submissions)

